Biophysical Chemistry 200–201 (2015) 48–55

Contents lists available at ScienceDirect

Biophysical Chemistry

journal homepage: http://www.elsevier.com/locate/biophyschem

Modulation of conformational changes in helix 69 mutants by pseudouridine modifications

Jun Jiang, Daya Nidhi Kharel, Christine S. Chow *

Department of Chemistry, Wayne State University, Detroit, MI 48202, United States

HIGHLIGHTS

- Pseudouridine (Ψ) modulates pH-dependent structural changes of helix 69 (H69) RNAs.
- Mutant A1912G requires Ψs for pH-dependent structural changes in H69 loop region.
- A1919G mutation leads to formation of a U/Ψ1911• G1919 wobble pair.
- G1919 and Ψ modifications work synergistically to modulate H69 structural changes.
- U1917C mutation leads to pH-dependent changes in the H69 loop and stem regions.

GRAPHICAL ABSTRACT

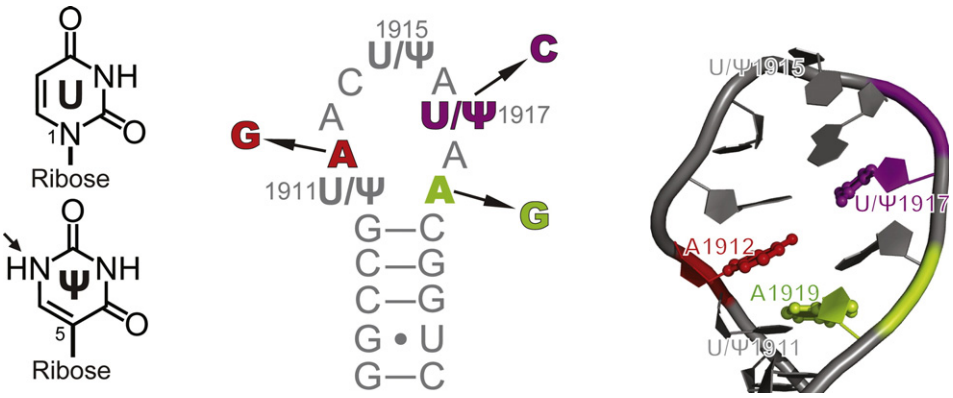

ARTICLE INFO

Article history:
Received 25 January 2015
Received in revised form 2 March 2015
Accepted 2 March 2015
Available online 11 March 2015

Keywords:
Ribosome
RNA
NMR
CD
Thermodynamics

ABSTRACT

Centrally located at the ribosomal subunit interface and mRNA tunnel, helix 69 (H69) from 23S rRNA participates in key steps of translation. Ribosome activity is influenced by three pseudouridine modifications, which modulate the structure and conformational behavior of H69. To understand how H69 is affected by the presence of pseudouridine in combination with sequence changes, the biophysical properties of wild-type H69 and representative mutants (A1912G, U1917C, and A1919G) were examined. Results from NMR and circular dichroism spectroscopy indicate that pH-dependent structural changes of wild-type H69 and the chosen mutants are modulated by pseudouridine and loop sequence. The effects of the mutations on global stability of H69 are negligible; however, pseudouridine stabilizes H69 at low pH conditions. Alterations to induced conformational changes of H69 likely result in compromised function, as indicated by previous biological studies.

1. Introduction

As the universally conserved machinery for protein synthesis, ribosomes play an indispensible role in the survival of all living organisms [1]. The ribosome is composed of two subunits, small and large, associated through multiple intersubunit bridges [2,3]. At the subunit interface, the mRNA molecule snakes through the ribosome, in concert with binding of tRNAs at the aminoacyl (A), peptidyltransferase (P), and exit (E) sites [4]. Within this region, helix 69 (H69) (Fig. 1), a 19-nucleotide hairpin located in domain IV of the 23S rRNA (large subunit RNA), establishes intersubunit bridge B2a with helix 44 (h44) of the 16S rRNA (small subunit RNA), and participates in the formation of intersubunit bridge B2b with helix 24 (h24) of the 16S rRNA [5]. Due

* Corresponding author. Tel.: +1 313 577 2594.
E-mail address: cchow@wayne.edu (C.S. Chow).

http://dx.doi.org/10.1016/j.bpc.2015.03.001
0301-4622/

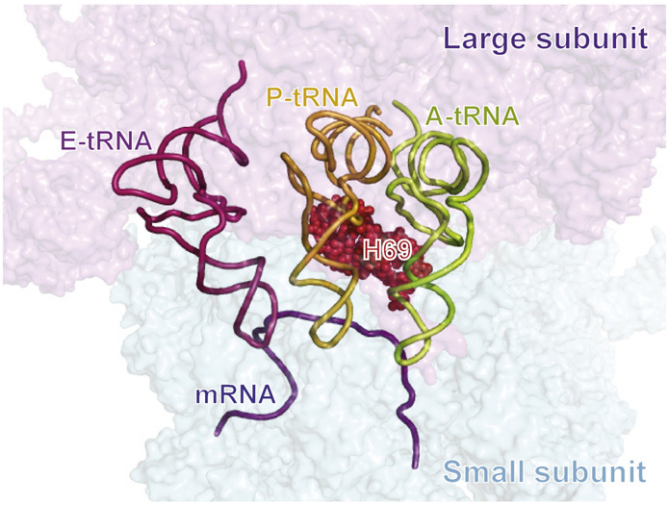

Fig. 1. The location of H69 within the 70S bacterial ribosome. The figure was prepared from the PDB IDs: 3I8F and 3I8G using PyMol [4]. As part of the large ribosomal subunit, H69 is located at the interface between the large and small subunits, and positioned between the A-site and P-site tRNAs. The tRNAs, together with the mRNA, move from right to left during the translation process, as illustrated in the figure.

to its central location in the ribosome, H69 is involved in almost every step of translation, in addition to ribosome rescue and antibiotic binding [6].

X-ray crystallography and solution-state nuclear magnetic resonance (NMR) spectroscopy revealed that bacterial (*Escherichia coli*) H69 assumes a hairpin structure, with a stem composed of five base pairs and a single-stranded loop of nine nucleotides [7,8], which is also observed in eukaryotic H69 [9]. Similarity in the 3D structures was deduced by high conservation and covariance of H69 sequences throughout phylogeny (Fig. 2a) [10]. In addition, pseudouridine (Ψ) modifications at loop positions 1911, 1915, and 1917 (*E. coli* numbering) are also conserved across the three kingdoms [11–15]. In this work, pseudouridylated H69 and the corresponding unmodified (uridine-containing) RNA will be referred to as ΨΨΨ and UUU, respectively. Uridine is isomerized to Ψ by replacing the *N1–C1′* glycosidic bond with a *C5–C1′* linkage (Fig. 2b). In *E. coli*, a single pseudouridine synthase, RluD, catalyzes this conversion at all three nucleotides in H69 [16]. The Ψ modifications have been shown to modulate structure and conformational behavior of H69 by stabilizing the loop-closing base pair and promoting base stacking in the 3′ half of the loop [8]. In *E. coli* H69, no net effects on hairpin stability due to Ψ modifications were observed at neutral pH. Previous studies showed that slight destabilizing effects of Ψ1915 and Ψ1917 canceled the stabilizing effects of Ψ1911 [17].

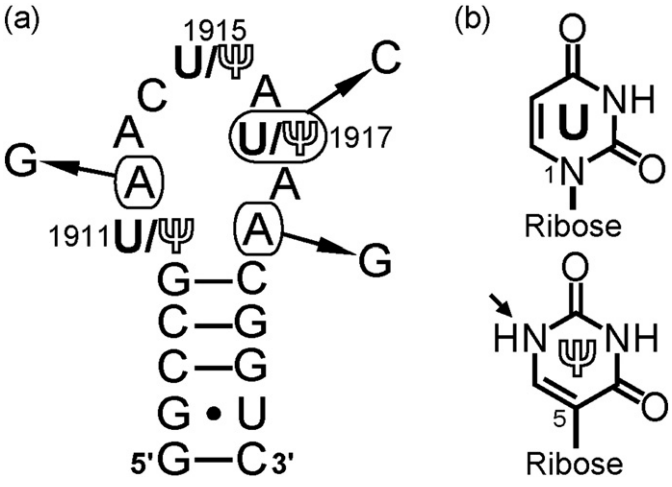

Fig. 2. Secondary structure of H69 and chemical structures of uridine (U) and pseudouridine (Ψ). a) Pseudouridine (Ψ) modifications at positions 1911, 1915, and 1917 (*E. coli* numbering) are labeled. The mutations employed in this project (*i.e.*, A1912G, U/Ψ1917C, and A1919G) are indicated with arrows, and the complete RNA sequences are listed in the Supplementary Information, Table S1. b) Due to replacement of the *N1–C1′* glycosidic bond by a *C5–C1′* linkage, the *N1*-position in Ψ is protonated (indicated by an arrow) and available for hydrogen-bonding interactions.

Conformational modulation by Ψ was discovered by examining pH sensitivity of the H69 structure [18,19]. More specifically, an A1913 stacked structure with protection from solvent (referred to as the "closed" conformation) was observed only in pseudouridylated H69 at low pH (5.5). In contrast, an alternate structure occurred at high pH (7.0), with increased exposure of A1913 ("open" conformation) [20,21]. These structures were proposed to be correlated with different conformational states of H69 during translation and establishment of intersubunit bridge B2a in complete ribosomes [18,19]. Pseudouridine modifications in H69 are not essential for bacterial growth under normal conditions [22]; however, loss of these modifications is disadvantageous for the growth of yeast under certain environmental challenges [23].

Extensive mutagenesis studies were done to identify functionally important residues of H69, especially within the loop region [24–29]. Mutations A1912G, A1919G, U/Ψ1917C were lethal to *E. coli* [24]. Furthermore, A1912, U1917, and A1919 were included in the functional sequences selected from randomized rRNA libraries [25]. Mutations at A1912 and A1919 did not affect pseudouridylation of H69 [26], but A1912G and A1919G caused compromised ribosome assembly, lower growth rates *in vivo*, and decreased *in vitro* protein synthesis activity of ribosomes [24], which correlated with reduced processivity of translation [30]. Similar effects were observed with the U/Ψ1917C mutant [24], which did not block pseudouridylation at positions 1911 and 1915 [26].

This work is focused on the biophysical properties of small RNAs representing the wild-type sequence and mutants (A1912G, U/Ψ1917C, and A1919G) of bacterial (*E. coli*) H69 with and without Ψ modifications. For the wild-type sequence and mutants with Ψ modifications, pH-dependent structural changes in the loop region are observed by NMR spectroscopy. These structural changes are not correlated with global RNA stability. However, at low pH conditions (5.5), a modest stabilizing effect from Ψ modification is observed in all cases, suggesting that pseudouridylation facilitates the folding of H69 and its mutants into energetically favorable conformational states. In some cases, the structural effects of the loop mutations propagate into the stem regions. These effects on structure are unique to each mutation, and influenced by Ψ modifications to different extents. These data suggest that Ψ modifications are capable of modulating the induced conformational changes of wild-type and mutant H69 RNAs, with some loop mutations causing additional conformational effects in the stem region, therefore explaining how loop mutations in conjunction with Ψ modifications result in functionally compromised ribosomes and decreased cell viability.

2. Materials and methods

The wild-type sequences (referred to as UUU and ΨΨΨ for the unmodified and modified constructs, respectively) and the modified mutant RNA oligonucleotides (ΨΨΨ-A1912G, ΨΨC-Ψ1917C, and ΨΨΨ-A1919G) representing H69 were purchased from Dharmacon® (Thermo Scientific) and purified by HPLC as described previously [8]. Unmodified mutant RNA oligonucleotides (UUU-A1912G, UUC-U1917C, and UUU-A1919G) RNA oligonucleotides were synthesized by *in vitro* T7 RNA polymerase transcription, and treated with calf-intestinal phosphatase (CIP) to remove the 5′ triphosphate moiety on the transcripts [31]. Twenty percent (*w*/*v*) denaturing polyacrylamide gels were used to purify the RNA transcripts and CIP-treated samples.

The final RNA oligonucleotides were characterized by MALDI-TOF mass spectrometry. The sequences are listed in the Supplementary Information (Table S1).

A Bruker AVANCE-AQS 700 MHz NMR spectrometer equipped with a TXI cryoprobe was employed to obtain the NMR spectra of all samples at 15 °C. Each RNA sample was dissolved in a buffer consisting of 250 μL of 10 mM phosphate (pH 5.5 or 7.0), 50 mM KCl in 9:1 H_2O/D_2O to a final concentration of 50 μM. The water suppression was achieved using WATERGATE 5 with a gradient pulse sequence [32]. Digital Quadratic detection for 16,000 data points was used to acquire the one-dimensional proton ($1D^1H$) NMR spectra, and 512 scans were collected to improve the signal-to-noise ratio.

Circular dichroism (CD) experiments were carried out on a Chirascan™ CD spectrometer from Applied Photophysics. A buffer consisting of 15 mM cacodylic acid (pH 5.5 or 7.0), 70 mM ammonium chloride, and 30 mM potassium chloride was employed. The extinction coefficients for pairs of unmodified and modified RNA oligonucleotides are as follows: 187,000 $Lmol^{-1}\ cm^{-1}$ (wild-type), 184,800 $Lmol^{-1}\ cm^{-1}$ (A1912G), 184,800 $Lmol^{-1}\ cm^{-1}$ (U/Ψ1917C), and 184,900 $Lmol^{-1}\ cm^{-1}$ (A1919G), at 260 nm [33]. The concentrations of the samples were about 13 μM. The CD spectra were collected from 220 to 320 nm at 23 °C in quadruplicate.

The thermal melting experiments were performed on a Beckman Coulter DU® 800 spectrophotometer equipped with temperature controller, multi-cell cuvette holder, and high-performance transport. The RNA samples (2 to 16 μM) were dissolved in a buffer containing 20 mM cacodylic acid (pH 5.5 or 7.0), 15 mM NaCl, and 0.5 mM Na_2EDTA. The absorbance at 280 nm of each sample was measured from 10 to 95 °C. The concentration of each sample was calculated using the UV absorbance ($\lambda = 260$ nm) at 90 °C and corresponding extinction coefficient. Meltwin 3.5 was used to derive the thermodynamic parameters assuming a two-state model [34].

3. Results and discussion

3.1. Pseudouridine modifications modulate pH-dependent structural changes of the H69 wild-type sequence and A1912G mutant

Crystal structures of complete ribosomes and individual subunits reveal that H69 adopts different conformational states during the translation process [35–39]. The conformational flexibility of H69 is believed to be important for optimal ribosomal activity. While exploring how H69 structure adapts under different solution environments and the role of Ψ modifications in this modulation, it was discovered through CD spectroscopy that pH variation could be used to promote Ψ-dependent conformational changes of this RNA motif [18]. Results from chemical probing experiments on ribosomal 50S subunits were consistent with those findings [20]. Modulation of the H69 conformational behavior by pseudouridylation is believed to result from a combination of enhanced base-stacking and hydrogen-bonding interactions unique to the Ψ-containing RNA, as determined by direct comparison of the solution structures of unmodified (UUU) and modified (ΨΨΨ) H69s [8]. Fully modified H69 containing *N3*-methylpseudouridine ($m^3Ψ$) at position 1915 (referred to as $Ψm^3ΨΨ$) was used in the initial pH-dependence studies, in which a two-state equilibrium model was proposed [18]. To confirm that pseudouridylation in the absence of methylation at position 1915 has the capability to modulate the pH-dependent structural changes, a modified H69 (ΨΨΨ) containing only the Ψ modifications at residues 1911, 1915, and 1917 was employed in CD and NMR experiments.

First, the CD spectra of ΨΨΨ at pH 7.0 and 5.5 (Supplementary Information, Fig. S1a) were compared. Both spectra have a peak maximum around 263 nm and a local peak minimum at 230 nm, with a crossover point around 240 nm, indicating a general A-form RNA structure (Table 1) [17,18]. Characteristic shifts of the CD profile are also observed when the pH is lowered from 7.0 to 5.5. An increase in molar ellipticity occurs from 235 to 251 nm with a concomitant decrease between 251 and 265 nm, which gives rise to an isosbestic point at 251 nm. The crossover point is shifted from 241 to 239 nm, and the peak maximum moves from 262 to 264 nm. The trends observed in this study are identical to those observed previously with $Ψm^3ΨΨ$ [18], suggesting that the ΨΨΨ construct undergoes pH-dependent structural changes similar to those of the fully modified RNA.

Table 1
Peak maxima, minima, and crossover points in the CD.

Name	pH	Peak maxima	Peak minima	Crossover	Isosbestic point
H69ΨΨΨ	7.0	262	–	241	265, 251
	5.5	264	–	239	
UUU-A1912G	7.0	265	–	248	263, 238
	5.5	266	–	249	
ΨΨΨ-A1912G	7.0	262	–	241	261, 249
	5.5	266	–	239	
UUU-A1919G	7.0	260	–	241	259, 241
	5.5	263	–	241	
ΨΨΨ-A1919G	7.0	253	–	237	–
	5.5	256	–	237	
UUC-U1917C	7.0	265	235	247	259, 247, 231
	5.5	266	–	247	
ΨΨC-Ψ1917C	7.0	267	234	246	270, 228
	5.5	266	–	245	

– not observed.

To explore more details of the pH-dependent structural changes of ΨΨΨ in comparison to the corresponding unmodified RNA, UUU, imino proton regions of the $1D^1H$ NMR spectra of UUU and ΨΨΨ at pH 7.0 and 5.5 were compared (Supplementary Information, Fig. S1b–e). The stem imino proton resonances (low field) are not shifted by more than 0.1 ppm with different modification status (UUU and ΨΨΨ) or pH conditions [8,40]. Compared to the spectra of UUU, an extra resonance corresponding to Ψ1911N1H (10.2 ppm) is apparent in the ΨΨΨ spectrum at pH 7.0 [8,17], as well as a peak from Ψ1915N1H (10.6 ppm) at pH 5.5 (Supplementary Information Fig. S2a, b) [40]. The resonance patterns in the ΨΨΨ spectra at different pH conditions are very similar to those of $Ψm^3ΨΨ$ [18], indicating that Ψ modifications are capable of modulating the pH-dependent structural behavior of the H69 loop in the absence of $m^3Ψ1915$.

Pseudouridine modifications have similar effects on the A1912G mutant H69 RNA. As shown in Fig. 3, the CD spectra of UUU-A1912 at pH 5.5 and 7.0 are almost completely overlapping. In contrast, an increase in molar ellipticity between 261 and 305 nm is observed with decreasing pH for the corresponding pseudouridylated mutant ΨΨΨ-A1912G. In this case, the peak maximum is red shifted from 262 (pH 7.0) to 266 nm (pH 5.5) (Table 1), compared to a 2 nm red shift for the pseudouridylated wild-type sequence (ΨΨΨ) with decreasing pH (Supplementary Information, Fig. S1a). These observations suggest that Ψ modifications are necessary for pH-dependent structural changes of the A1912G mutant, and the nucleotide composition also plays a role in this event. In support of this hypothesis, no change in chemical shifts or peak intensities is observed in the NMR spectra of UUU-A1912G when the pH condition is changed (Fig. 3c, d). In the NMR spectra of ΨΨΨ-A1912G (Fig. 3e, f), resonances corresponding to the ΨN1H protons (Supplementary Information Fig. S2c, d) are clearly observed, with peak patterns similar to those of ΨΨΨ (Supplementary Information, Fig. S1d, e). A difference worth noting is that the relative peak intensities of the ΨN1H protons compared to the stem imino proton resonances in the spectra of ΨΨΨ-A1912G are higher than those of the ΨΨΨ RNA. This observation suggests that G1912 may have specific effects on the Ψ- and pH-dependent structural changes in the H69 loop region that differ slightly from those in ΨΨΨ. More specifically, hydrogen-bonding interactions involving the corresponding ΨN1H protons appear to be enhanced. These pH-dependent differences in the CD and NMR spectra of ΨΨΨ and ΨΨΨ-A1912G might appear

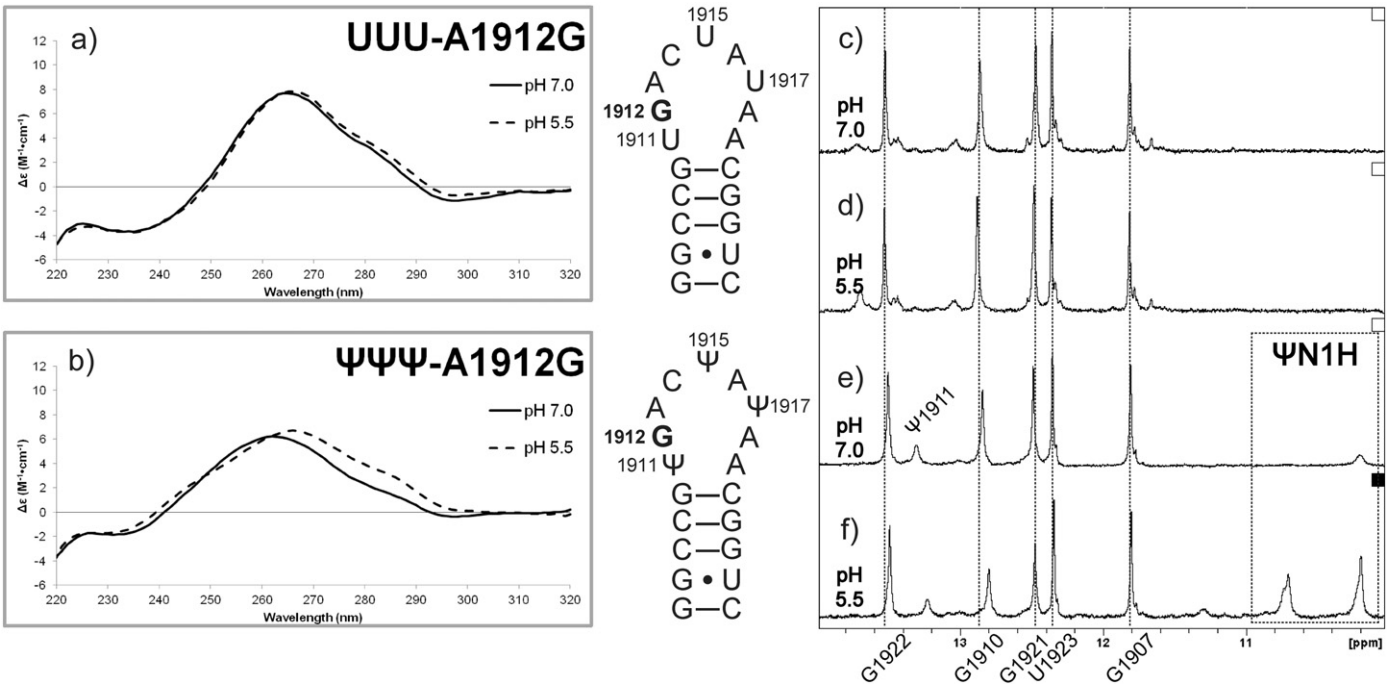

Fig. 3. CD and NMR spectra of the unmodified and modified H69 A1912G mutants. The CD spectra of UUU- and ΨΨΨ-A1912G at pH 7.0 (solid line) and pH 5.5 (dashed line) are given in panels a and b, respectively. The NMR spectra of unmodified (UUU, c and d) and modified (ΨΨΨ, e and f) A1912G were obtained at pH 7.0 (c and e) or pH 5.5 (d and f) as indicated.

small; however, unique conformational states or alterations in H69 dynamics have the potential to impact the RNA function such that the A1912G mutation is lethal to *E. coli* [24,30].

3.2. Pseudouridine modifications and A1919G mutation work synergistically to modulate the pH-dependent structural changes of ΨΨΨ-A1919G

In previous studies, pseudouridylation at position 1911 was shown to have an impact on the thermodynamics, structure, and conformational behavior of H69 by establishing a stable Watson–Crick base pair with A1919 and a hydrogen-bonding interaction specific to RNAs with a Ψ1911 residue [8,17,41]. These results suggest that the H69 loop structure and conformational behavior are sensitive to the modification status of the loop-closing base pair, which may in turn impact ribosomal function.

Besides the modification status, nucleotide composition of the loop-closing base pair may also play a role in modulating the H69 loop conformational behavior. We therefore tested the A1919G mutants for

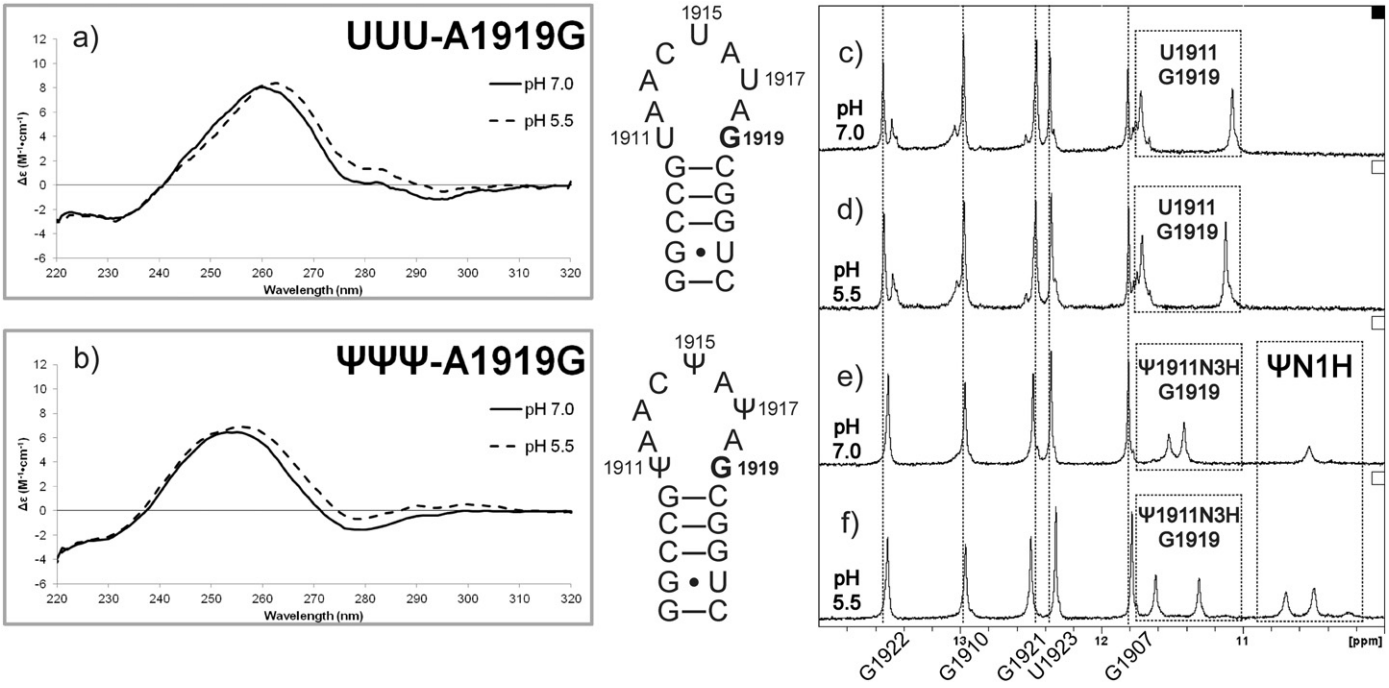

Fig. 4. CD and NMR spectra of the unmodified and modified H69 A1919G mutants. The CD spectra of UUU- and ΨΨΨ-A1919G at pH 7.0 (solid line) and pH 5.5 (dashed line) are given in panels a and b, respectively. The NMR spectra of unmodified (UUU, c and d) and modified (ΨΨΨ, e and f) A1919G were obtained at pH 7.0 (c and e) or pH 5.5 (d and f) as indicated.

pH-dependent structural changes. As shown in Fig. 4a and b, the global peak maxima for both UUU-A1919G and ΨΨΨ-A1919G are red shifted by 3 nm (Table 1) when the pH is lowered from 7.0 to 5.5, and there is a concomitant increase in molar ellipticity between the peak maxima and 310 nm. These observations suggest that the A1919G mutation plays a role in the pH-dependent structural changes of these RNAs, even in the absence of Ψ.

Structural effects of the A1919G mutation are further revealed in 1D ^{1}H NMR spectra (Fig. 4c–f). For UUU-A1919G (Fig. 4c, d), the same imino proton resonances as with UUU are observed (Supplementary Information, Fig. S1b, c), along with two extra imino proton peaks at 11.1 and 11.7 ppm. These peaks are assigned as U1911N3H and G1919N1H in a U•G wobble pair, based on NOE difference spectroscopy [17]. In the same region (Fig. 4e, f), two peaks from Ψ1911N3H and G1919N1H (Supplementary Information Fig. S3) are observed in the ΨΨΨ-A1919G spectra. Formation of a Ψ1911•G1919 wobble pair results in a 0.3 ppm downfield shift of the Ψ1911N1H resonance (Supplementary Information Fig. S2e–g) in both spectra (pH 7.0 and 5.5), compared to those from ΨΨΨ (Supplementary Information, Fig. S1d, e). Even though no difference in either chemical shift or peak pattern is observed in the UUU-A1919G spectra at different pH conditions (Fig. 4c, d), the possibility should not be excluded that there is a pH-dependent structural change in the UUU-A1919G loop region, as suggested by the CD spectra (Fig. 4a). Structural effects in the UUU-A1919G loop (*e.g.*, base stacking or solvent exposure of nucleotide bases) do not necessarily alter hydrogen-bonding interactions. In contrast, when the pH is decreased from 7.0 to 5.5, changes in the chemical shifts of the Ψ1911N3H and G1919N1H imino protons and extra imino proton resonance in the loop region are observed for ΨΨΨ-A1919G (Fig. 4e, f). These spectral changes reveal that the presence of Ψ extends the pH-dependent structural changes of A1919G beyond the loop single-stranded residues to include the loop-closing base pair Ψ1911•G1919. The mutated 1919 residue (G) and Ψ modifications appear to work synergistically to modulate the pH-dependent structural changes of ΨΨΨ-A1919G, which differ from ΨΨΨ. Such changes could be detrimental to the translation steps that require proper conformational-state adjustments, especially in the single-stranded loop and loop-closing base pair of H69.

3.3. The U/Ψ1917C mutation affects pH-dependent structural changes of H69

The U1917 residue of H69 shows 100% conservation across phylogeny [10], and Ψ modification at this position has been detected in all species whose rRNA pseudouridylation sites are currently known [11]. The important functional role of Ψ1917 is also revealed in ribosome assays. A Ψ1917C mutation was shown to decrease cellular polysome levels and cause a strong growth defect [24], even though Ψ modifications at sites other than 1917 were unlikely affected [26]. The importance of Ψ1917 can be attributed to its structural roles. As observed in NMR solution studies on UUU and ΨΨΨ, Ψ1917 mediates base-stacking interactions in the 3' half of the ΨΨΨ loop region [8]. Residue Ψ1917 is also suggested to participate in formation of the B2a intersubunit bridge by hydrogen bonding to A1912 in complete ribosomes [2]. To reveal the effects of U/Ψ1917C on H69 structure and pH-dependent structural changes, CD and NMR experiments were employed.

As shown in Fig. 5a and b, a decrease in molar ellipticity between 275 and 310 nm is observed in both unmodified (UUC-U1917C) and modified (ΨΨC-Ψ1917C) mutant H69 RNAs, when the pH is lowered from 7.0 to 5.5. No shift in the peak maxima is demonstrated in either UUC-U1917C or ΨΨC-Ψ1917C. Similar spectral features shared by the unmodified and modified U/Ψ1917C mutants, along with differences identified between ΨΨC-Ψ1917C and ΨΨΨ spectra (Supplementary Information, Fig. S1a), indicate that nucleotide composition of the loop may play a dominant role in determining the pH-dependent structural changes in U/Ψ1917C H69 RNAs.

The hypothesis that nucleotide composition at position 1917 plays a role in mediating H69 structural changes is supported by NMR data (Fig. 5c–f). At pH 7.0, all five signature imino proton resonances from the H69 stem region are observed (Fig. 5c, e). In contrast, only four sharp peaks are visible when the pH is lowered to 5.5 (Fig. 5d, f).

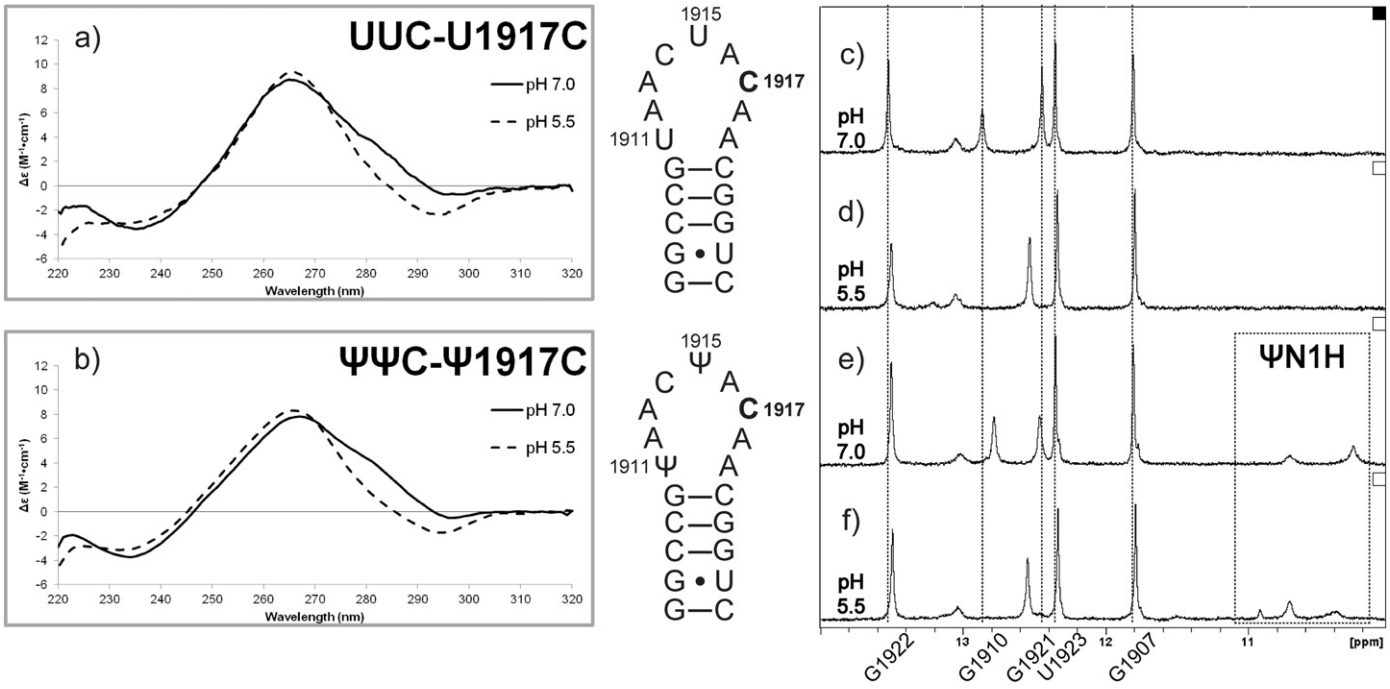

Fig. 5. CD and NMR spectra of the unmodified and modified H69 U/Ψ1917C mutants. The CD spectra of UUC- and ΨΨC-U/Ψ1917C at pH 7.0 (solid line) and pH 5.5 (dashed line) are given in panels a and b, respectively. The NMR spectra of unmodified (UUC, c and d) and modified (ΨΨC, e and f) U/Ψ1917C were obtained at pH 7.0 (c and e) or pH 5.5 (d and f) as indicated.

These observations suggest that pH-dependent structural changes of the U/Ψ1917C mutants are extended into the stem regions, and the G1910•C1920 stem-closing base pair is destabilized at pH 5.5. Accompanying the loss of G1910•C1920 base pairing, the proton resonance corresponding to G1921N1H is downfield shifted by 0.1 ppm, and the peak intensities are decreased. This structural change at lower pH common to both U/Ψ1917C mutants may account for the similar trend in pH-induced changes of the CD spectra (Fig. 5a, b). The Ψ1917C mutation also causes changes in the H69 structure at neutral pH. The peak most likely corresponding to Ψ1911N1H in the ΨΨC-Ψ1917C spectrum (Fig. 5e) is upfield shifted by 0.1 ppm compared to that of ΨΨΨ (Supplementary Information, Fig. S1a). The resonance pattern in the upfield (ΨN1H) imino proton region of ΨΨC-Ψ1917C at pH 5.5 is also very different from that of ΨΨΨ. Since Ψ1917 and Ψ1911 do not have direct interactions in either the solution structure of ΨΨΨ [8] or X-ray crystal structures of complete ribosomes [36], the difference in spectral features between ΨΨC-Ψ1917C and ΨΨΨ at both pH conditions potentially results from an altered structure of the ΨΨC-Ψ1917C loop region caused by the mutation. Long-range effects of the U/Ψ1917C mutation on the stem-region structure, which are independent of the Ψ modifications, suggest stem-loop crosstalk [19,41]. Mutations at key loop residues, such as 1917, involved in mediating this crosstalk, may also be responsible for monitoring interactions with the P-site tRNA and other translational factors, *e.g.*, A-site tRNA or release factors (RFs), in complete ribosomes [27–29,42], and therefore responsible for lethality in *E. coli*.

3.4. The pH-dependent structural changes of H69 and mutants are not correlated to alteration in global stability

A change in stability of an RNA molecule may be correlated to either a structural adaptation or altered conformational flexibility, although not all conformational changes lead to altered RNA stability because of the enthalpy-entropy compensation [43]. In a previous study with the Ψm^{3}ΨΨ construct, the RNA was stabilized by −0.5 kcal/mol when the pH was lowered from 7.0 to 5.5, which was accompanied by CD spectral changes [18]. In thermal melting experiments with ΨΨΨ, the difference in stability at the two pH values is only −0.2 kcal/mol (Table 2), negligible when the expected standard error (0.2 kcal/mol) is considered. As discussed in Section 3.1 (CD experiments), the conformational changes of ΨΨΨ with pH variation closely resemble those of Ψm^{3}ΨΨ. The minor differences could be attributed to *N3*-methylation on Ψ1915 in Ψm^{3}ΨΨ, contributing to the modestly enhanced stabilizing effects [18]. Taken together, these results suggest that the Ψ modifications are responsible for the pH-dependent structural changes of ΨΨΨ, but have minimal or no effects on the global stability of ΨΨΨ at different pH conditions. Similar small differences in Gibbs free energy between unmodified and modified RNAs are observed with the H69 mutants (Table 2), indicating that Ψ modifications confer conformational effects without altering the global stability as the solution pH is changed. The thermodynamic parameters for the mutants are listed in the Supplementary Information (Table S1).

Even though modest or negligible differences in the thermal stabilities of the RNA constructs are observed with varying pH conditions ($\Delta G^\circ_{37\text{pH }5.5} - \Delta G^\circ_{37\text{pH }7.0}$), Ψ modifications are shown to slightly stabilize the global folding of H69 and mutants at pH 5.5 compared to pH 7.0 (Table 2). A $\Delta\Delta G^\circ_{37}$ ($\Delta G^\circ_{37\Psi\Psi\Psi} - \Delta G^\circ_{37\text{UUU}}$) value of −0.5 kcal/mol is observed for H69 (Supplementary Information Fig. S4a) and mutants A1912G and U/Ψ1917C. This value matches that of a previous thermal melting study with Ψm^{3}ΨΨ [18]. These results suggest that Ψ modifications dominate the stabilizing effects of certain conformational states of H69 and the loop mutants. The hypothesis is supported by fluorescence studies employing modified H69 with 2-aminopurine (2AP) at position 1913, in which the fluorescence intensity from 2AP in ΨΨΨ decreased at pH 5.5 relative to 7.0 due to enhanced base stacking of 2AP1913 with neighboring bases [19]. A similar change was not observed with 2AP-containing UUU, suggesting that the modification plays a role in the conformational switch. As discussed previously, A1913 plays important roles in establishing the intersubunit bridge B2a [2,5]. Therefore, the conformational response of A1913 in Ψ- and pH-dependent structural changes of H69 may contribute to the growth advantage of living organisms [23].

Stabilizing effects of pseudouridylation are also observed for the A1919G mutant, with $\Delta\Delta G^\circ_{37}$ ($\Delta G^\circ_{37\Psi\Psi\Psi} - \Delta G^\circ_{37\text{UUU}}$) values of −0.9 kcal/mol (pH 5.5, Supplementary Information Fig. S4b) and −0.4 kcal/mol (pH 7.0, Supplementary Information Fig. S4c), respectively (Table 2). The larger $\Delta\Delta G^\circ_{37}$ values for A1919G compared to other H69 mutants suggest that the sequence alteration in combination with Ψ modifications impacts the H69 structure. Furthermore, the largest free energy difference is observed at pH 5.5, implying that G1919 plays a different role than A1919 in modulating H69 conformational states. Position 1919 is unique in mediating the structural effects of Ψ modifications. In the NMR structure of ΨΨΨ, A1919 forms a Watson–Crick base pair with Ψ1911, as well as mediates base-stacking interactions on the 3′ side of the H69 loop from Ψ1915 to A1919, which is promoted by modified nucleotides Ψ1915 and Ψ1917 [8]. Similar to A1919 in ΨΨΨ, G1919 may also mediate structural effects of the Ψ modifications within ΨΨΨ-A1919G. As shown by NMR spectroscopy, pH-dependent structural changes of ΨΨΨ-A1919G involve the formation, as well as changes in imino proton chemical shifts, of a Ψ1911•G1919 wobble pair. The synergistic modulations of G1919 and Ψ modifications, resulting from the sequence and structural contexts in which they reside, appear to cause a more significant impact on conformational-state modulation of H69, which in turn elicits biological effects that differ from ΨΨΨ or the other H69 mutants.

4. Conclusions

Helix 69 plays important roles in the assembly of ribosomes and protein synthesis process [6]. Conservation of Ψ modifications at positions

Table 2
Comparison of ΔG°_{37} values of H69 and mutants.

Name	pH 7.0		pH 5.5		Δ pH
	ΔG°_{37} (kcal/mol)	$\Delta\Delta G^\circ_{37}$ (kcal/mol) ($\Delta G^\circ_{37\Psi\Psi\Psi} - \Delta G^\circ_{37\text{UUU}}$)	ΔG°_{37} (kcal/mol)	$\Delta\Delta G^\circ_{37}$ (kcal/mol) ($\Delta G^\circ_{37\Psi\Psi\Psi} - \Delta G^\circ_{37\text{UUU}}$)	$\Delta\Delta G^\circ_{37}$ (kcal/mol) ($\Delta G^\circ_{37\text{pH }5.5} - \Delta G^\circ_{37\text{pH }7.0}$)
UUU	−4.6 ± 0.1	−0.1 ± 0.2	−4.4 ± 0.1	−0.5 ± 0.2	0.2 ± 0.2
ΨΨΨ	−4.7 ± 0.1		−4.9 ± 0.1		−0.2 ± 0.2
UUU-A1912G	−4.7 ± 0.1	−0.2 ± 0.2	−4.7 ± 0.1	−0.5 ± 0.2	0.0 ± 0.2
ΨΨΨ-A1912G	−4.9 ± 0.1		−5.2 ± 0.1		−0.3 ± 0.2
UUC-U1917C	−4.4 ± 0.1	−0.3 ± 0.2	−4.4 ± 0.1	−0.5 ± 0.2	0.0 ± 0.2
ΨΨC-Ψ1917C	−4.7 ± 0.1		−4.9 ± 0.1		−0.2 ± 0.2
UUU-A1919G	−4.3 ± 0.1	−0.4 ± 0.2	−4.0 ± 0.1	−0.9 ± 0.2	0.3 ± 0.2
ΨΨΨ-A1919G	−4.7 ± 0.1		−4.9 ± 0.1		−0.2 ± 0.2

The thermodynamic effects of Ψ modifications and pH were determined as the free energy difference ($\Delta\Delta G^\circ_{37}$).

1911, 1915, and 1917 are suggested to be correlated to their functions in modulating the structures and conformational behaviors of H69 [8,17–21,41,44]. Results from the work presented here reveal that both Ψ modifications and the lethal mutations, A1919G and U/Ψ1917C, are capable of modulating pH-dependent structural changes of H69 independently. In the modified H69 lethal mutants, the mutated residue may also work synergistically with the Ψ modifications to introduce additional structural effects. For example, A1912G appears to alter hydrogen-bonding interactions at lower pH, but only in the presence of loop Ψ residues. Within a different sequence and structural context, the same mutation of A to G has an altered role. The A1919G mutation leads to formation of a loop-closing Ψ1911•G1919 wobble pair that appears to modulate the H69 loop structure with pH and modification status, but does not impact the stem structure. In contrast, the Ψ1917C mutant expands the pH-dependent structural changes from the loop region into the stem G1910•C1920 base pair. These pH-dependent structural changes do not affect the global thermal stability of H69 RNAs, but modest stabilizing effects of Ψ modifications are consistently observed at pH 5.5. These results suggest that stabilization of certain conformational states of H69 is inherent to Ψ modifications, possibly through alterations in hydrogen-bonding and/or base stacking interactions involving Ψ residues. As with the wild-type H69 construct and full-length 23S rRNA, the changes in conformational states of the RNA can be induced by lowering the solution pH to 5.5. These changes occur due to protonation of nucleotides that are yet to be identified, but likely to be conserved within the loop of H69. Furthermore, NMR spectral evidence of the stem-loop crosstalk within H69 is directly observed in pH-dependent structural changes of U/Ψ1917C, consistent with suggestions in the literature that H69 may not simply form simultaneous contacts with the A- or P-site tRNAs [38] or RFs [39,45], but instead plays a role in coordinating the activities of the tRNAs and RFs [27–29,42].

Given the essential functions of H69 in translation and the multiple conformational states observed in structure studies, alterations in the structural changes of H69 by mutations may lead to the phenotypes observed in the functional analyses. Knowledge gained in this project from pH-induced structural changes of H69 extends our understanding of the effects of post-translational modifications and interplay with mutations on the structure and conformational behavior of these RNAs. In addition, modulation of the structure and pH-dependent structural changes of H69 by ligand binding may serve as an effective pathway to design and screen antibiotics targeting bacterial protein synthesis.

Acknowledgments

The authors thank Dr. A. Feig for assistance with the circular dichroism experiments and the Lumigen Instrument Center for supporting the 700 MHz NMR facility. This project was funded by NIH [GM087596].

Appendix A. Supplementary data

Supplementary data to this article can be found online at http://dx.doi.org/10.1016/j.bpc.2015.03.001.

References

[1] K.H. Nierhaus, D.N. Wilson, Protein Synthesis and Ribosome Structure: Translating the Genome, WILEY-VCH, Weinheim, 2004.
[2] B.S. Schuwirth, M.A. Borovinskaya, C.W. Hau, W. Zhang, A. Vila-Sanjurjo, J.M. Holton, J.H.D. Cate, Structures of the bacterial ribosome at 3.5 Å resolution, Science 310 (5749) (2005) 827–834, http://dx.doi.org/10.1126/science.1117230.
[3] A. Ben-Shem, L. Jenner, G. Yusupova, M. Yusupov, Crystal structure of the eukaryotic ribosome, Science 330 (6008) (2010) 1203–1209, http://dx.doi.org/10.1126/science.1194294.
[4] L.B. Jenner, N. Demeshkina, G. Yusupova, M. Yusupov, Structural aspects of messenger RNA reading frame maintenance by the ribosome, Nat. Struct. Mol. Biol. 17 (5) (2010) 555–560, http://dx.doi.org/10.1038/nsmb.1790.
[5] A. Liiv, M. O'Connor, Mutations in the intersubunit bridge regions of 23 S rRNA, J. Biol. Chem. 281 (40) (2006) 29850–29862, http://dx.doi.org/10.1074/jbc.M603013200.
[6] J. Jiang, Y. Sakakibara, C.S. Chow, Helix 69: a multitasking RNA motif as a novel drug target, Isr. J. Chem. 53 (6–7) (2013) 379–390, http://dx.doi.org/10.1002/ijch.201300012.
[7] J. Harms, F. Schluenzen, R. Zarivach, A. Bashan, S. Gat, I. Agmon, H. Bartels, F. Franceschi, A. Yonath, High resolution structure of the large ribosomal subunit from a mesophilic eubacterium, Cell 107 (5) (2001) 679–688, http://dx.doi.org/10.1016/S0092-8674(01)00546-3.
[8] J. Jiang, R. Aduri, C.S. Chow, J. Santalucia Jr., Structure modulation of helix 69 from *Escherichia coli* 23S ribosomal RNA by pseudouridylations, Nucleic Acids Res. 42 (6) (2014) 3971–3981, http://dx.doi.org/10.1093/nar/gkt1329.
[9] S. Klinge, F. Voigts-Hoffmann, M. Leibundgut, S. Arpagaus, N. Ban, Crystal structure of the eukaryotic 60S ribosomal subunit in complex with initiation factor 6, Science 334 (6058) (2011) 941–948, http://dx.doi.org/10.1126/science.1211204.
[10] J.J. Cannone, S. Subramanian, M.N. Schnare, J.R. Collett, L.M. D'Souza, Y. Du, B. Feng, N. Lin, L.V. Madabusi, K.M. Müller, N. Pande, Z. Shang, N. Yu, R.R. Gutell, The comparative RNA web (CRW) site: an online database of comparative sequence and structure information for ribosomal, intron, and other RNAs, BMC Bioinf. 3 (2) (2002)http://dx.doi.org/10.1186/1471-2105-3-2.
[11] J. Ofengand, Ribosomal RNA pseudouridines and pseudouridine synthases, FEBS Lett. 514 (1) (2002) 17–25, http://dx.doi.org/10.1016/S0014-5793(02)02305-0.
[12] J. Ofengand, A. Bakin, Mapping to nucleotide resolution of pseudouridine residues in large subunit ribosomal RNAs from representative eukaryotes, prokaryotes, archaebacteria, mitochondria and chloroplasts, J. Mol. Biol. 266 (2) (1997) 246–268, http://dx.doi.org/10.1006/jmbi.1996.0737.
[13] A. Baudin-Baillieu, C. Fabret, X.H. Liang, D. Piekna-Przybylska, M.J. Fournier, J.P. Rousset, Nucleotide modifications in three functionally important regions of the *Saccharomyces cerevisiae* ribosome affect translation accuracy, Nucleic Acids Res. 37 (22) (2009) 7665–7677, http://dx.doi.org/10.1093/nar/gkp816.
[14] M. Del Campo, C. Recinos, G. Yanez, S.C. Pomerantz, R. Guymon, P.F. Crain, J.A. McCloskey, J. Ofengand, Number, position, and significance of the pseudouridines in the large subunit ribosomal RNA of *Haloarcula marismortui* and *Deinococcus radiodurans*, RNA 11 (2) (2005) 210–219, http://dx.doi.org/10.1261/rna.7209905.
[15] J. Mengel-Jørgensen, S.S. Jensen, A. Rasmussen, J. Poehlsgaard, J.J.L. Iversen, F. Kirpekar, Modifications in *Thermus thermophilus* 23 S ribosomal RNA are centered in regions of RNA–RNA contact, J. Biol. Chem. 281 (31) (2006) 22108–22117, http://dx.doi.org/10.1074/jbc.M600377200.
[16] S. Raychaudhuri, J. Conrad, B.G. Hall, J. Ofengand, A pseudouridine synthase required for the formation of two universally conserved pseudouridines in ribosomal RNA is essential for normal growth of *Escherichia coli*, RNA 4 (11) (1998) 1407–1417.
[17] M. Meroueh, P.J. Grohar, J. Qiu, J. SantaLucia Jr., S.A. Scaringe, C.S. Chow, Unique structural and stabilizing roles for the individual pseudouridine residues in the 1920 region of *Escherichia coli* 23S rRNA, Nucleic Acids Res. 28 (10) (2000) 2075–2083, http://dx.doi.org/10.1093/nar/28.10.2075.
[18] S.C. Abeysirigunawardena, C.S. Chow, pH-dependent structural changes of helix 69 from *Escherichia coli* 23S ribosomal RNA, RNA 14 (4) (2008) 782–792, http://dx.doi.org/10.1261/rna.779908.
[19] Y. Sakakibara, S.C. Abeysirigunawardena, A.-C.E. Duc, D.N. Dremann, C.S. Chow, Ligand- and pH-induced conformational changes of RNA domain helix 69 revealed by 2-aminopurine fluorescence, Angew. Chem. Int. Ed. 51 (48) (2012) 12095–12098, http://dx.doi.org/10.1002/anie.201206000.
[20] Y. Sakakibara, C.S. Chow, Probing conformational states of modified helix 69 in 50S ribosomes, J. Am. Chem. Soc. 133 (22) (2011) 8396–8399, http://dx.doi.org/10.1021/Ja2005658.
[21] Y. Sakakibara, C.S. Chow, Role of pseudouridine in structural rearrangements of helix 69 during bacterial ribosome assembly, ACS Chem. Biol. 7 (5) (2012) 871–878, http://dx.doi.org/10.1021/cb200497q.
[22] M. O'Connor, S.T. Gregory, Inactivation of the RluD pseudouridine synthase has minimal effects on growth and ribosome function in wild-type *Escherichia coli* and *Salmonella enterica*, J. Bacteriol. 193 (1) (2011) 154–162, http://dx.doi.org/10.1128/JB.00970-10.
[23] X.-H. Liang, Q. Liu, M.J. Fournier, rRNA modifications in an intersubunit bridge of the ribosome strongly affect both ribosome biogenesis and activity, Mol. Cell 28 (6) (2007) 965–977, http://dx.doi.org/10.1016/j.molcel.2007.10.012.
[24] A. Liiv, D. Karitkina, Ü. Maiväli, J. Remme, Analysis of the function of *E. coli* 23S rRNA helix-loop 69 by mutagenesis, BMC Mol. Biol. 6 (18) (2005)http://dx.doi.org/10.1186/1471-2199-6-18.
[25] N. Hirabayashi, N.S. Sato, T. Suzuki, Conserved loop sequence of helix 69 in *Escherichia coli* 23 S rRNA is involved in A-site tRNA binding and translational fidelity, J. Biol. Chem. 281 (25) (2006) 17203–17211, http://dx.doi.org/10.1074/jbc.M511728200.
[26] M. Leppik, L. Peil, K. Kipper, A. Liiv, J. Remme, Substrate specificity of the pseudouridine synthase RluD in *Escherichia coli*, FEBS J. 274 (21) (2007) 5759–5766, http://dx.doi.org/10.1111/j.1742-4658.2007.06101.x.
[27] R.F. Ortiz-Meoz, R. Green, Helix 69 is key for uniformity during substrate selection on the ribosome, J. Biol. Chem. 286 (29) (2011) 25604–25610, http://dx.doi.org/10.1074/jbc.M111.256255.
[28] M. O'Connor, Helix 69 in 23S rRNA modulates decoding by wild type and suppressor tRNAs, Mol. Genet. Genomics 282 (4) (2009) 371–380, http://dx.doi.org/10.1007/s00438-009-0470-6.
[29] M. O'Connor, A.E. Dahlberg, The involvement of two distinct regions of 23 S ribosomal RNA in tRNA selection, J. Mol. Biol. 254 (5) (1995) 838–847, http://dx.doi.org/10.1006/jmbi.1995.0659.
[30] K. Kipper, C. Hetényi, S. Sild, J. Remme, A. Liiv, Ribosomal intersubunit bridge B2a is involved in factor-dependent translation initiation and translational processivity, J. Mol. Biol. 385 (2) (2009) 405–422, http://dx.doi.org/10.1016/j.jmb.2008.10.065.

[31] C. Huang, Y.-T. Yu, Synthesis and labeling of RNA in vitroChapter 4 Curr. Protoc. Mol. Biol. Unit 4 (15) (2013)http://dx.doi.org/10.1002/0471142727.mb0415s102.
[32] T.-L. Hwang, A.J. Shaka, Water suppression that works. Excitation sculpting using arbitary waveforms and pulsed field gradients, J. Magn. Reson. Ser. A 112 (1995) 275–279, http://dx.doi.org/10.1006/jmra.1995.1047.
[33] E.G. Richards, Use of tables in calculation of absorption, optical rotary dispersion, and circular dichroism of polyribonucleotides, in: 3rd edn, G.D. Fasman (Ed.) Handbook of Biochemistry and Molecular Biology: Nucleic Acids, vol. 1, CRC Press, Cleveland, 1975, pp. 596–603.
[34] J.A. McDowell, D.H. Turner, Investigation of the structural basis for thermodynamic stabilities of tandem GU mismatches: solution structure of (rGAGGUCUC)2 by two-dimensional NMR and simulated annealing, Biochemistry 35 (45) (1996) 14077–14089, http://dx.doi.org/10.1021/bi9615710.
[35] G. Blaha, R.E. Stanley, T.A. Steitz, Formation of the first peptide bond: the structure of EF-P bound to the 70S ribosome, Science 325 (5943) (2009) 966–970, http://dx.doi.org/10.1126/science.1175800.
[36] J.A. Dunkle, L. Wang, M.B. Feldman, A. Pulk, V.B. Chen, G.J. Kapral, J. Noeske, J.S. Richardson, S.C. Blanchard, J.H. Cate, Structures of the bacterial ribosome in classical and hybrid states of tRNA binding, Science 332 (6032) (2011) 981–984, http://dx.doi.org/10.1126/science.1202692.
[37] A.H. Ratje, J. Loerke, A. Mikolajka, M. Brünner, P.W. Hildebrand, A.L. Starosta, A. Dönhöfer, S.R. Connell, P. Fucini, T. Mielke, P.C. Whitford, J.N. Onuchic, Y. Yu, K.Y. Sanbonmatsu, R.K. Hartmann, P.A. Penczek, D.N. Wilson, C.M.T. Spahn, Head swivel on the ribosome facilitates translocation by means of intra-subunit tRNA hybrid sites, Nature 468 (7324) (2010) 713–716, http://dx.doi.org/10.1038/nature09547.
[38] T.M. Schmeing, R.M. Voorhees, A.C. Kelley, Y.G. Gao, F.V. Murphy IV, J.R. Weir, V. Ramakrishnan, The crystal structure of the ribosome bound to EF-Tu and aminoacyl-tRNA, Science 326 (5953) (2009) 688–694, http://dx.doi.org/10.1126/science.1179700.
[39] A. Weixlbaumer, H. Jin, C. Neubauer, R.M. Voorhees, S. Petry, A.C. Kelley, V. Ramakrishnan, Insights into translational termination from the structure of RF2 bound to the ribosome, Science 322 (5903) (2008) 953–956, http://dx.doi.org/10.1126/science.1164840.
[40] J.-P. Desaulniers, Y.-C. Chang, R. Aduri, S.C. Abeysirigunawardena, J. SantaLucia Jr., C.S. Chow, Pseudouridines in rRNA helix 69 play a role in loop stacking interactions, Org. Biomol. Chem. 6 (21) (2008) 3892–3895, http://dx.doi.org/10.1039/b812731j.
[41] M. Sumita, J. Jiang, J. SantaLucia Jr., C.S. Chow, Comparison of solution conformations and stabilities of modified helix 69 rRNA analogs from bacteria and human, Biopolymers 97 (2) (2012) 94–106, http://dx.doi.org/10.1002/bip.21706.
[42] P.V. Baranov, R.F. Gesteland, J.F. Atkins, P-site tRNA is a crucial initiator of ribosomal frameshifting, RNA 10 (2) (2004) 221–230, http://dx.doi.org/10.1261/rna.5122604.
[43] K.A. Dill, Additivity principles in biochemistry, J. Biol. Chem. 272 (2) (1997) 701–704, http://dx.doi.org/10.1074/jbc.272.2.701.
[44] M. Sumita, J.-P. Desaulniers, Y.-C. Chang, H.M. Chui, L. Clos II, C.S. Chow, Effects of nucleotide substitution and modification on the stability and structure of helix 69 from 28S rRNA, RNA 11 (9) (2005) 1420–1429, http://dx.doi.org/10.1261/rna.2320605.
[45] A. Korostelev, J. Zhu, H. Asahara, H.F. Noller, Recognition of the amber UAG stop codon by release factor RF1, EMBO J. 29 (15) (2010) 2577–2585, http://dx.doi.org/10.1038/emboj.2010.139.